View metadata, citation and similar papers at core.ac.uk
brought to you by CORE
provided by Apollo

Supplementary Information:

Fast, Non-Contact, Wafer-Scale, Atomic Layer Resolved Imaging of 2D Materials by Ellipsometric Contrast Micrography

Philipp Braeuninger-Weimer[1*], Sebastian Funke[2*], Ruizhi Wang[1], Peter Thiesen[2], Daniel Tasche[3], Wolfgang Viöl[3], Stephan Hofmann[1]

1 Department of Engineering, University of Cambridge, Cambridge CB3 0FA, UK
2 Accurion GmbH, Stresemannstraße 30, Göttingen, Germany
3 University of Applied Sciences and Arts, Faculty of Natural Sciences and Technology, Von-Ossietzky-Straße 99, Göttingen, Germany

* These authors contributed equally to the manuscript

Supplementary data to the manuscript:

Section 1: Additional Raman Data

In addition to Figure 3(a) in the main text Figure S1 shows the Raman map for various other graphene Raman signatures. Figure S1(a) shows the ratio of 2D/G peak intensities. Two white arrows indicate areas of bilayer graphene (see microscope picture in the main text Figure 3(b)). Although these are both bilayer graphene regions both regions show a different 2D/G ratio which arises due to different rotations between the first and second graphene layer.[1] The same is true for the full width half maximum (FWHM) of the 2D peak, 2D intensity, 2D peak position and G peak position which are all affected by the rotational alignment between bilayers. The G peak intensity appears to be least affected by rotational alignment and can therefore be used by itself to clearly distinguish between layer number. However, peak intensity is also dependent on how well the sample is focused and the underlying substrate and would need to be calibrated with a reference sample if the G peak intensity is to be used as a direct indicator of layer number.

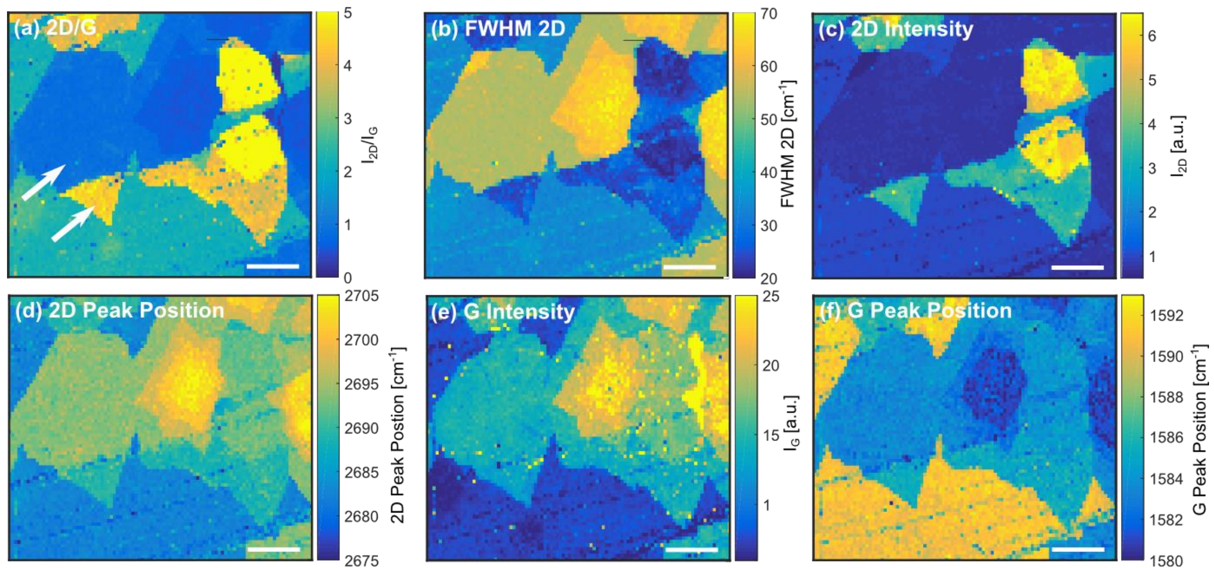

Figure S1: Raman maps for the "Raman Area" in Figure 3 in the main text. (a) Map for the 2D/G peak intensity ratio, (b) map of the full width half maximum (FWHM) of the 2D peak, (c) map of the 2D peak intensity, (d) map of the 2D peak position, (e) G peak intensity and (f) G peak position map. All scalars are 50 μm.

Figure S2 shows a Raman spectrum acquired at location (II) shown in Figure 7(b) in the main text. The spectrum shows a peak at position ~1370 cm^{-1} which corresponds to monolayer h-BN.[2]

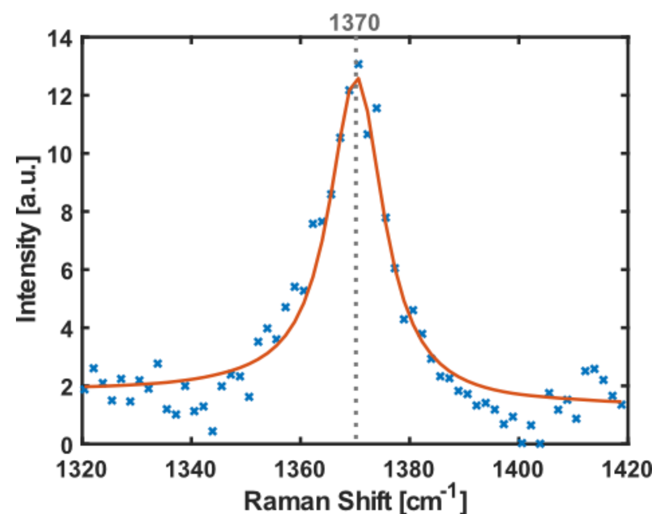

Figure S2: Raman signature of h-BN transferred on Si/SiO_2 substrate

Section 2: Choice of Ellipsometer Parameters for h-BN and Graphene

When optimising the contrast of a 3 component system of Si/SiO_2 substrate, graphene and h-BN the contrast of all possible combination needs to be considered. Again to simplify the optimisation we a priori set λ = 550 nm, AOI = 60° and C = 45°. To find the optimum contrast of all 4 regions shown in Figure 7(b) we measure an optical rotation of P and A on the 4 regions (see Figure S3 (a)-(d)). Next, we set a minimum threshold intensity of 100 counts

and find the *P* and *A* setting that maximises the contrast between the 4 regions by considering the standard deviation of the region where all differences in intensities are higher than 100 counts (Fig. S3(e)). The visualization of the regions where a minimum contrast of 100 counts of all regions is given in Figure S3 (f). The optimal setting is found for *P* = 161° and *A* = 57°.

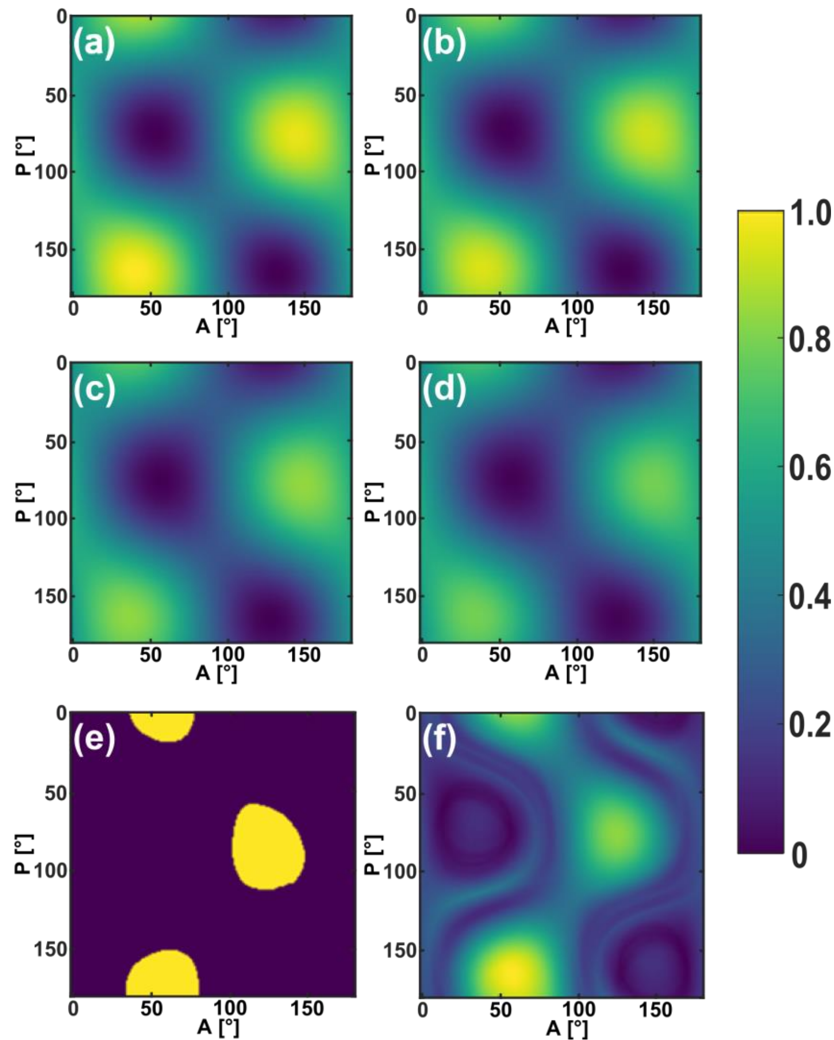

Figure S3: Normalized intensities measured for a *P* and *A* rotation on (a) Si/SiO_2, (b) Si/SiO_2/h-BN, (c) Si/SiO_2/graphene (d) Si/SiO_2/h-BN/graphene. (e) (yellow) pixels declare regions where all differences in intensities for all regions are higher than 100 counts. (f) Standard deviation of all differences in intensities. Maximum in contrast is found for the highest standard deviation where all differences in intensities are higher than 100 counts.

Section 3: Extracting Quantitative Values and Artefacts

When determining layer number, 2D material contrast, coverage and level of surface contamination the resulting measurement error is linked to the contrast difference between the different layers/contamination/uncovered regions. To illustrate this, we show in Figure S4 the contrast histograms of the images shown in Figure 3.

Figure S4 (a) shows that for Raman mapping the G peak intensity for 1 and 2 layers of graphene can be well distinguished and can be fitted with Gaussian-Lorentzian curves. However, the G peak intensity difference between 2 and more layers is less pronounced, and the fitted peaks are broader and overlap. Consequently, it is more difficult to distinguish 2 or more layers by simply mapping the G peak intensity. For optical microscopy where we plot the R-channel contrast in Figure S4 (b) 1, 2 and 3 layers can be distinguished. For more than 3 layers the fitted curves overlap which corresponds to an intensity where an unambiguous distinction in layer number cannot be made. We note that for optical microscopy optimised protocols for this task exists that may overcome this limitation.[3] *Δ*-Mapping provides the best contrast between layers as can be seen by the well separated peaks in Figure S4 (c), where each peak corresponds to a different layer number and the signal can be fitted by a Gauss-Lorentz curve without overlap. ECM (using λ = 450 nm, AOI = 50°, P = 50°, A = 9°, C = 45°) also offers good contrast between 1, 2 and 3 layers (Figure S4 (d)), whereas again the contrast is less well defined for 4-6 layers. The choice of ECM parameters can be used to increase the separation of the peaks and thereby optimise the contrast between different graphene layer thicknesses.

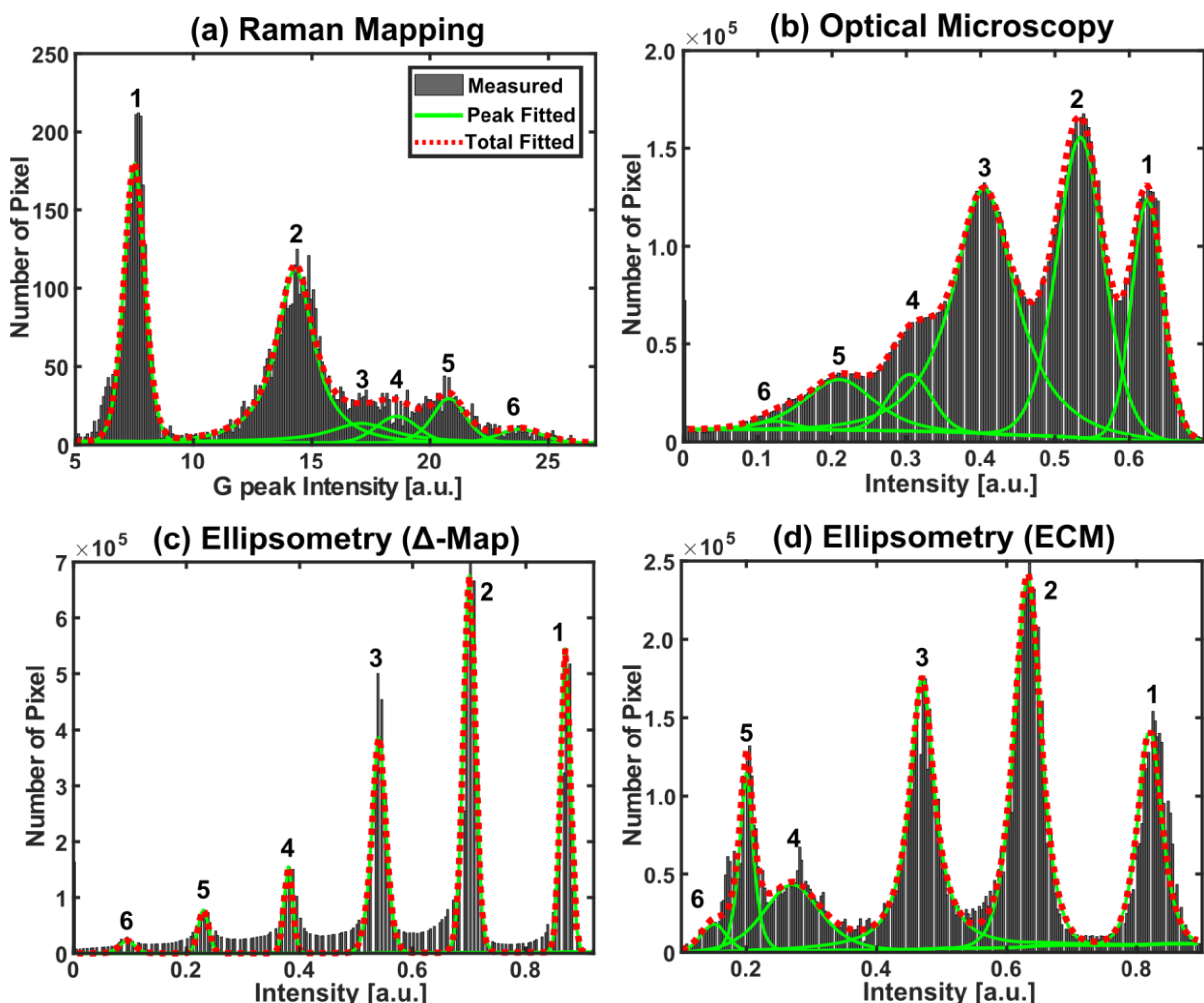

Figure S4: Histogram of the contrast for the images shown in Figure 3 in the main text. The labels 1, 2, …, 6 correspond to the graphene layer number, the grey boxes correspond to the number of occurrences of this intensity, the green lines

correspond to fitted curves and the red dotted line to the overall fit. (a) Histogram for the Raman map as shown in Figure 3(a), (b) histogram for the optical microscopy image shown in Figure 3(b), (c) histogram for the *Δ*-map shown in Figure 3(c) and (d) histogram for the ECM shown in Figure 3(d).

Using the area under the fitted peaks we estimate the respective coverage of 1-6 layers and the results are shown in Table S1. Note that the area used for Raman mapping is different than for the other cases and thus different area coverage values are obtained.

Table S1: Percentage layer coverage from peak fitting as shown in Figure S4 for Raman mapping, optical microscopy, ellipsometry *Δ*-mapping and ECM.

	1-Layer	2-Layers	3-Layers	4-Layers	5-Layers	6-Layers
Raman	27 %	35 %	12 %	9 %	11 %	7 %
Microscope	16 %	27 %	32 %	9 %	11 %	6 %
Δ-Map	24 %	35 %	24 %	7 %	5 %	3 %
ECM	17 %	29 %	25 %	13 %	10 %	6 %

Figure S5 shows the contrast histograms for the ECM measurements in Figure 5, Figure 6 and Figure 7 in the main text. On Si and Cu the ECM contrast between graphene and substrate is less pronounced than on Si/SiO_2 resulting in more overlap of the respective peaks in the histogram plot. Similarly, for the Si/SiO_2 sample with monolayer graphene and h-BN where the layers can be distinguished from each other and the substrate, but some overlap is found.

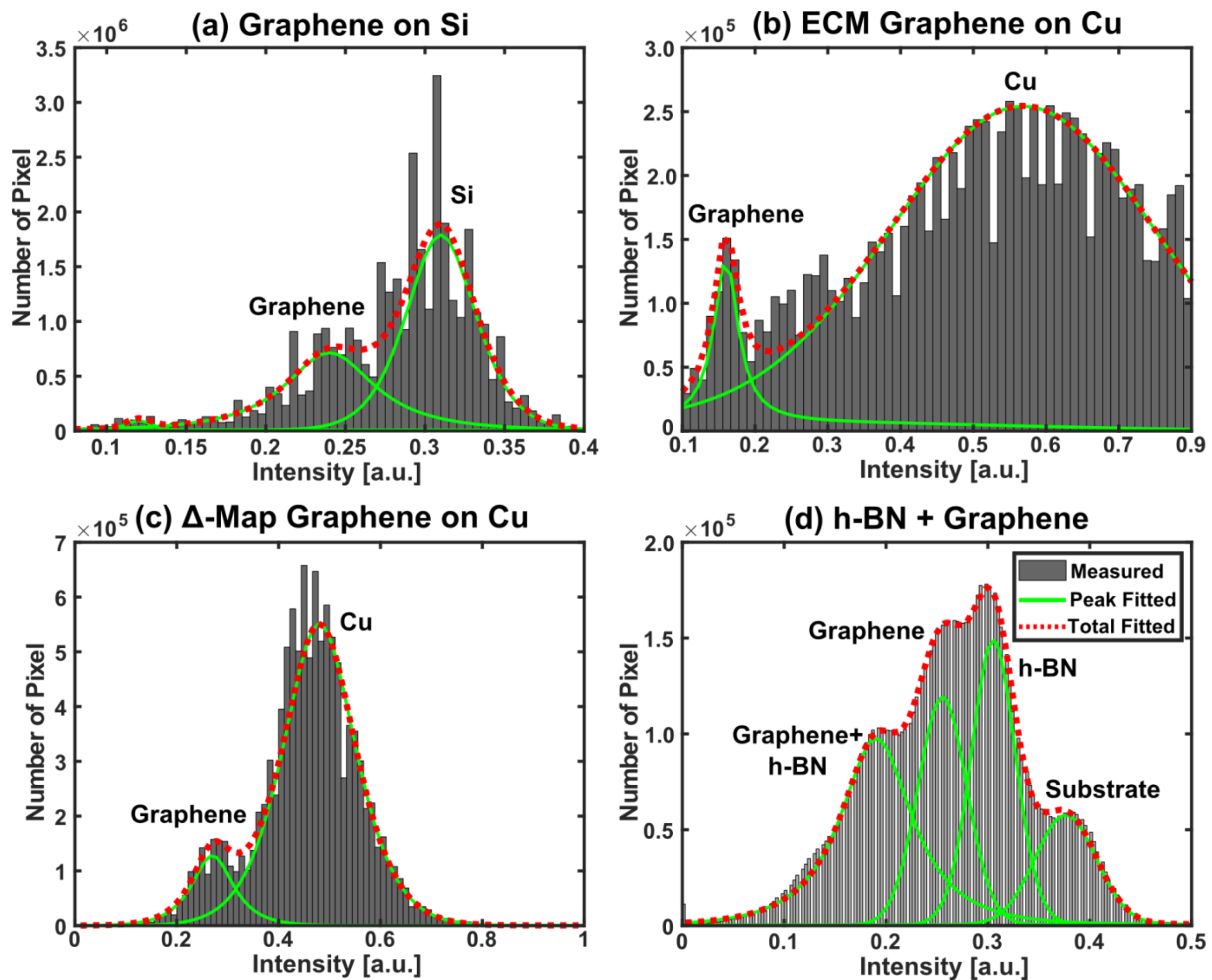

Figure S5: Histogram for (a) graphene on Si measured by ECM, (b) graphene on Cu foil measured by ECM, (c) *Δ*-map of graphene on Cu foil and (d) ECM of monolayer h-BN and monolayer graphene on Si/SiO_2.

When mapping very large areas as shown in Figure 5 we also observe some intensity artefact that can be correlated to a small tilt of the sample as well as stitching related artefacts as shown by an arrow in Figure S6 (a). Figure S6 (a) shows in black the intensity region 0.15-0.26 that from Figure S5 (a) can be associated to graphene. Besides the graphene area in the centre other areas on the wafer not covered with graphene show the same ECM intensity which are artefacts from sample tilt, stitching and contamination. Figure S6 (b) shows the Cu rolling striation induced artefact when thresholding for graphene (intensity range: 0.01-0.25) in ECM measurement. This artefact is significantly less pronounced in the *Δ*-map (intensity range: 0.01-0.31). We note that the quantitative results could be improved with software packages that perform background correction, filter for rolling striations and correct stitching artefacts.

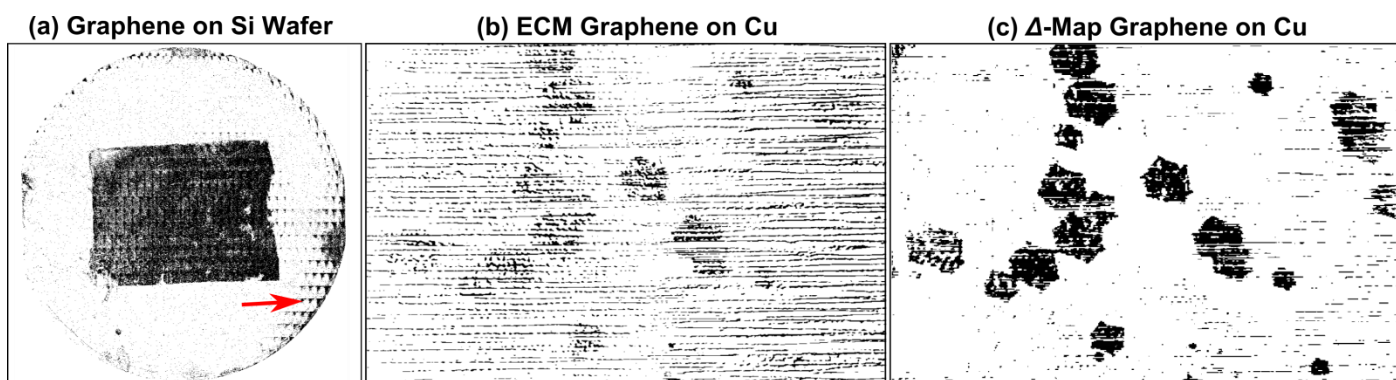

Figure S6: Intensity thresholding for graphene covered regions, showing graphene in black. (a) ECM of graphene on Si, the red arrow indicates stitching related artefacts (b) ECM of graphene on Cu foil and (c) the *Δ*-map of graphene on Cu.

Section 4: Detecting and Characterising Polymer Contamination

The graphene transfer procedure can result in a thin layer of polymer contamination covering the graphene layer. If this polymer film is homogeneously covering the graphene layer it will not be visible as differential contrast in the ECM image unless a clean (*e.g.* exfoliated graphene) reference sample is used. However, imaging ellipsometry can be used to characterise the residual polymer contamination without a reference substrate. We exemplarily show this for the sample of graphene on a Si wafer shown in Figure 5 in the main text. Figure S7 shows the comparison of ECM and *Δ*-map, where in both cases obvious contamination can be easily distiguished. ECM is recorded for AOI = 60°, *P* = 94°, *C* = 45°, *A* = 139°, *λ* = 490 nm and *Δ*-map is acquired at AOI = 60° and *λ* = 480 nm. For the two areas shown in Figure S7(b) labelled *A* and *B*, the *Δ* spectra is shown in Figure S7(c). The areas *A* and *B* are representative of a location with obvious contamination and without obvious contamination, respectively. With the help of a model the thickness of the overlaying polymer contamination can be estimated. We adopt a model of recent publications using a layer of Poly(methyl methacrylate) (PMMA), the graphene layer and the substrate to extract the PMMA thickness.[4,5] For area *A* the best fit is obtained for a fitted PMMA thickness of 1.31 nm and for area *B* the best fit is obtained for 0.5 nm PMMA thickness.

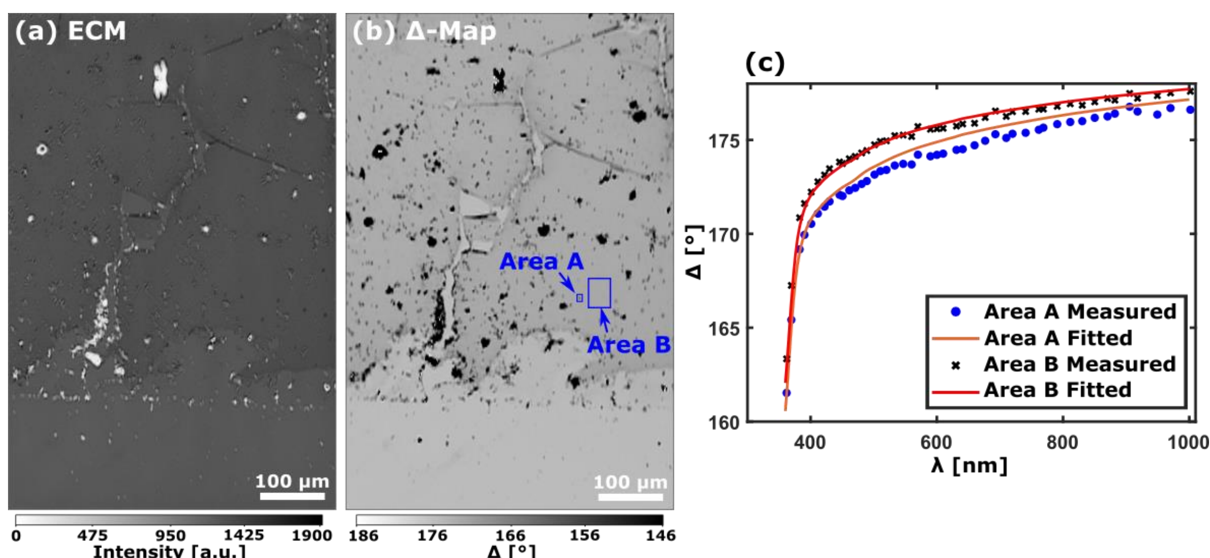

Figure S7: ECM (a) and *Δ*-map (b) of graphene transferred on a Si wafer. (c) Averaged *Δ* spectra for the areas marked *A* and *B* in (b), where *A* represents an area of obvious contamination and area *B* an area without obvious contamination on the graphene layer, respectively.

References

(1) Kim, K.; Coh, S.; Tan, L. Z.; Regan, W.; Yuk, J. M.; Chatterjee, E.; Crommie, M. F.; Cohen, M. L.; Louie, S. G.; Zettl, A. Raman Spectroscopy Study of Rotated Double-Layer Graphene: Misorientation-Angle Dependence of Electronic Structure. *Phys. Rev. Lett.* **2012**, *108*, 1–6.

(2) Gorbachev, R. V.; Riaz, I.; Nair, R. R.; Jalil, R.; Britnell, L.; Belle, B. D.; Hill, E. W.; Novoselov, K. S.; Watanabe, K.; Taniguchi, T.; Geim, A. K.; Blake, P. Hunting for Monolayer Boron Nitride: Optical and Raman Signatures. *Small* **2011**, *7*, 465–468.

(3) Jessen, B. S.; Whelan, P. R.; Mackenzie, D. M. A.; Luo, B.; Thomsen, J. D.; Gammelgaard, L.; Booth, T. J.; Bøggild, P. Quantitative Optical Mapping of Two-Dimensional Materials. *Sci. Rep.* **2018**, *8*, 1–23.

(4) Matkovic, A.; Beltaos, A.; Milicevic, M.; Ralevic, U.; Vasic, B.; Jovanovic, D.; Gajic, R. Spectroscopic Imaging Ellipsometry and Fano Resonance Modeling of Graphene. *J. Appl. Phys.* **2012**, *112*, 123523.

(5) Crovetto, A.; Whelan, P. R.; Wang, R.; Galbiati, M.; Hofmann, S.; Camilli, L. Non-Destructive Thickness Mapping of Wafer-Scale Hexagonal Boron Nitride down to a Monolayer. *ACS Appl. Mater. Interfaces* **2018**.